THESIS

APPLICATION OF FOURIER-TRANSFORMED-INFRARED SPECTROSCOPY TO QUANTITATE AMORPHOUS SILICA IN PERSONAL AIR SAMPLES IN SUGARCANE CUTTERS

Submitted by

Colton Castro

Department of Environmental and Radiological Health Sciences

In partial fulfillment of the requirements
For the Degree of Master of Science
Colorado State University
Fort Collins, Colorado
Spring, 2025

Master's Committee:

Advisor: Joshua Schaeffer

John Adgate
Jacqueline Chaparro

ABSTRACT

APPLICATION OF FOURIER-TRANSFORMED-INFRARED SPECTROSCOPY TO QUANTITATE AMORPHOUS SILICA IN PERSONAL AIR SAMPLES IN SUGARCANE CUTTERS

In recent years, chronic kidney disease of unknown origin (CKDu) has risen to an epidemic level in Latin America. Specifically, in agricultural communities of sugarcane cutters, the burden of the disease is unusually high. Several hypotheses exist as to the cause of the disease, focusing on various risk factors, including dehydration, nutrition, and thermal stress. Another important risk factor warranting further research is exposure to particulate matter (PM), given its nephrotoxic potential. PM can be defined as solid or liquid particles present in the environment, often microscopic. Sugarcane workers are exposed to high PM concentrations containing various contaminants, including amorphous silica. In sugarcane, the leaves and other excess plant material contain amorphous silica that can be released into the worker's environment during harvest. Quantitating this amorphous silica and determining if it can play a deleterious role in kidney health has become a priority. Still, amorphous silica is a challenging analyte that requires time- and cost-intensive analysis. A previous pilot project aimed to develop a predictive model using Fourier-Transformed-Infrared Spectroscopy (FTIR) to analyze amorphous silica non-destructively and cost-effectively compared to the currently accepted NIOSH method (e.g., X-ray diffraction). The model was created, and initial concentrations of amorphous silica were determined. During the analysis of samples, the need to ascertain the detection limit of the FTIR method was evident. This project, therefore, further aimed to evaluate and analyze amorphous silica using direct-on-filter FTIR spectroscopy. The

point of analysis where several discrepancies occurred (i.e., inconsistency with detecting the peak, loading amounts detected, etc.) was determined to be approximately 500 micrograms before the FTIR began to over or underestimate the absorbance values based on concentration changes. This study is one of the first attempts to use FTIR to non-destructively analyze and quantitate air sampling filters. Additionally, the results will be compared to the current limit of detection values for the FTIR methods employed by NIOSH for their silica analysis tool, further contributing to the literature.

ACKNOWLEDGEMENTS

I would like to thank Professor Joshua Schaeffer for his immense understanding, knowledge, and support in every aspect of this project. His guidance and development of the project were crucial to the work, and I would not have reached this stage without his support.

This research was funded with support from the CDC/NIOSH Mountain and Plains Education and Research Center (MAP ERC) and the National Institute of Environmental Health Sciences (NIEHS; 1R01ES031585)

I would also like to thank the committee for their understanding and expertise in revising and providing feedback during the completion of this Thesis.

Finally, I would like to thank my friends and family for supporting me while I was away on trips or in the lab a little too late. Their support helped me through the struggles and the triumphs of this process.

I would also like to thank Laura Calvimontes Barrientos for all her assistance in collecting the data, analyzing the data, and explaining how sugarcane processing works. This project would not have been possible without her input.

Additionally, I would like to thank Yin Htin Wang for her last-minute assistance on some final data collection and management.

TABLE OF CONTENTS

1. INTRODUCTION

Chronic Kidney Disease of Unknown Etiology (CKDu) is a disease with global implications among agricultural workers [1-10]. For example, CKDu affects rice farmers in southeastern Asia and is especially prevalent in sugarcane workers in Latin American countries [1-3,5]. In 2013, the Pan-American Health Organization declared CKDu a serious public health problem in Latin America [4]. Currently, sugarcane cutters in Guatemala are suffering from high rates of CKDu [1,3]. The challenge with CKDu is that it doesn't follow typical risk factors associated with kidney disease, such as diabetes and hypertension [1-3,5]. Further, the disease seems to affect young – otherwise healthy individuals in Central America. A myriad of proposed risk factors contribute to the disease, ranging from viral infections to chronic heat exhaustion and exposure to environmental toxins (i.e., pesticides, silica, heavy metals, etc.) [1-3.5].

Given the unknown nature and various hypotheses of CKDu's etiology in Latin America, recent studies have been conducted to confirm or eliminate different risk factors and assess the relative contribution of each to the disease [2]. Of these, environmental toxins are perhaps the least understood given the nature of each toxin (i.e., arsenic exposure via inhalation or ingestion vs. silica inhalation) [1]. A highly noted feature of sugarcane harvesting is the burning of the sugarcane before manual harvest. Estimates suggest that for every one hectare of sugarcane, 20000 kilograms of waste will be consumed, producing and releasing a high quantity of particulate matter (PM) into the air [11]. PM has been associated with pulmonary and kidney effects. However, further research into identifying specific chemicals in the inhaled particulate remains of interest to determine exposure risk [12,13].

A 2018 pilot study by Schaeffer et al. investigated the contribution of environmental contaminants to inhalation exposure among Guatemalan sugarcane workers, focusing mainly on minerals and heavy metals known to be harmful to kidneys [14]. The researchers collected

particulate matter of a diameter less than 2.5 micrometers and less than 100 micrometers and then analyzed their elemental composition [14]. Heavy toxic elements were below detectable levels. Intriguingly, they discovered the presence of silicon dioxide (or silica) in the samples [14]. However, inductively coupled mass spectroscopy and surface electron microscopy using energy-dispersive technology determined that the silica present was amorphous [14]. Considering Schaeffer and colleagues' results, coupled with Johnson and colleagues' review article that states there are little to no respiratory issues indicative of crystalline silica and its resulting disease, silicosis, the workers are likely exposed to the non-crystalline form, amorphous silica [1,11,15-21].

Amorphous silica has been poorly researched as crystalline silica's carcinogenic nature is most often cited in the literature [19]. For reference, when IARC released its monograph discussing crystalline and amorphous silica, only six studies were conducted on occupational exposure to either diatomaceous earth or biogenic silica fibers [19,23]. Further complicating the matter is quantifying amorphous silica as it does not diffract X-rays and is therefore analyzed via a laborious, cost-intensive, and destructive method [26]. Newer methods developed by NIOSH for crystalline silica involve using a Potassium Bromide (KBR) Pellet and Infrared Spectroscopy method for quantitation of silica [15,25]. More recently, NIOSH conducted a study to evaluate software that allows for the quantitation of crystalline silica using a portable FTIR, allowing industrial hygienists to conduct end-of-shift analyses for overexposure [27]. Most importantly, these analyses are non-destructive, leaving the filter intact, which provides for other analyses to be conducted on the filters for other contaminants of concern. These results were limited, however, to crystalline silica in mine settings, with no suggestions on the potential for amorphous silica analysis [27,29].

With the novelty of the NIOSH software and current limitations surrounding amorphous silica quantitation and its potential health effects, the objective of this study was to develop a predictive model using Fourier-Transformed Infrared Spectroscopy (FTIR) to quantify

amorphous silica present in the personal air samples collected from study participants at a sugarcane operation in Guatemala. We hypothesize that FTIR will be able to quantitate amorphous silica after creating a model to predict concentrations solely based on absorbance values using direct-on-filter (DOF) techniques.

2. REVIEW OF LITERATURE

2.1: Introduction to Kidney Disease, Prevalence of CKDu, and Hypotheses

Chronic Kidney Disease (CKD) is one of the most significant contributors to mortality worldwide, with estimates in 2017 of >840 million people suffering from the disease [30]. Further concerns about CKD include the correlation between CKD and age as global life expectancy increases [31]. Risk factors associated with CKD include diabetes, obesity, and hypertension, all of which are seeing an increase in prevalence [32]. While initially a problem in developed countries, CKD is increasing in prevalence in developing countries, especially in Latin America and Southeast Asia [30]. However, kidney disease in several regions (i.e., Sri Lanka in South Asia, Guatemala, Nicaragua, and El Salvador in Latin America) is reported to lack the risk factors attributed to CKD mentioned above [33-35]. In other words, the disease appears to be developing from an unknown cause in each region, and researchers coined the disease "Chronic Kidney Disease of Unknown Etiology (CKDu)" [1, 33-38]. The disease is concerning as the diagnosis often occurs in the later stages of the disease, requiring dialysis [36]. In developing countries, dialysis is not feasible due to the significant cost and advanced medical instrumentation required to treat patients [36]. This leads to a disproportionate burden of mortality placed on rural communities in developing countries where only 5-15% of patients will receive dialysis when it is required for survival [35]. Considering the severity of the disease and lack of adequate medical treatment in developing countries, organizations, including the Pan-American Health Organization, have declared CKDu in Latin America a serious public health problem [37]. Researchers have also labeled it as a global health concern [37, 38].

Consequently, significant efforts have been made by researchers to characterize and identify contributors to the disease in two primary regions: 1.) Sri Lanka and 2.) Latin America

[33-35,37,39-41]. Researchers sought to find commonalities that may partially explain the rise of CKDu in the two regions and be able to propose strategies to reduce the incidence rates present in these countries.

1.) Sri Lanka

Chronic Kidney Disease of Uncertain etiology was first reported in Sri Lanka in the 1990s when farmers presented with kidney disease but lacked traditional risk factors [33,41,42]. As of 2019, Alwis and Panawala estimated the prevalence rate to be 4.7% in the North Central Province, where the CKDu burden was unusually high [41]. In Sri Lanka, CKDu causative factors were hypothesized to include:

1.) Heavy metals (i.e., Cadmium, Arsenic, Lead, Aluminum, Chromium etc.) from drinking water exposure [33,39,42]
2.) Mycotoxins (i.e., Ochratoxin-A, Aflatoxins etc.) from consuming various medicinal herbs and foods grown in the region [39]
3.) Pesticide exposure (i.e., 2,4-D, glyphosate, and AMPA) during agricultural growing operations [33,39]

Of these, Rajapakse and colleagues (2016) determined that the risk factors are related to the environment and agriculture; however, any further determination of the causative agent remains to be made [39]. More recently, Kulathunga and colleagues (2019) conducted a review of the literature of CKDu in Sri Lanka and investigated low-level exposure to heavy metals in diseased individuals and concluded that even at low concentrations, heavy metals may interact and lead to nephrotoxic effects [42]. Similar to previous studies, these researchers also concluded that further investigation was required in Sri Lankan CKDu [42]. Collectively, researchers studying CKDu suggest that the major limitation of unraveling CKDu in Sri Lanka is often due to poor study design and mixed conclusions regarding the same exposure [33,39,42]. Other regions suffering from CKDu may provide more information that could help this region.

2.) Latin America (Meso-America)

An epidemic of CKDu was also discovered in Latin America during the 1990s [1,2]. It was noted that agricultural communities in this region suffered the highest burden. Specifically, sugarcane farmers on the Pacific coast were experiencing prevalence rates ranging between 18-41% [2]. In Latin America, the causative hypotheses for the high prevalence include:

1.) Heat stress due to increasing temperatures and high workloads resulting in dehydration [1,2]
2.) Heavy metals and other nephrotoxic agents (i.e., Arsenic, Cadmium, Lead, Silica etc.) during the harvest season [1,2,11]
3.) Pesticide exposure (i.e., glyphosate, organophosphates, carbamates etc.) during growing season and burning process [1]

Of these hypotheses, heat stress and heavy metals have recently emerged as the primary exposures contributing to CKDu. Johnson and colleagues (2019) present the major support and challenge for each of these exposures [1]. For example, silica exposure, a potential risk factor for CKDu, has supportive evidence of being present both in sugarcane and particulate matter during the harvest [1,11,17,20,21]. Continuing, Johnson and colleagues also present evidence that silica is not a risk factor since individuals with CKD do not present with pulmonary symptoms associated with silica exposure [1]. Heat stress is hypothesized to damage the kidneys via several mechanisms, including heat stroke and inflammatory responses, dehydration leading to hyperosmolality, and heat exposure leading to rhabdomyolysis [1,2,43,44,45]. Particulate matter with nephrotoxic chemicals (i.e., heavy metals, silica, etc.) is also a potential contributor to CKDu [11,14]. The mechanism for CKDu via PM involves inhalation or ingestion, resulting in transport to the proximal tubule, where damage occurs as metabolization occurs and translocation across the cell layers occurs [11,14,19,20]. Research is ongoing, with evidence that both hypotheses contribute to the development of CKDu amongst workers in Latin America. Extensive research has begun investigating the

potential nephrotoxic agents present in the particulate matter the workers are exposed to, which will be the primary exposure investigated in my thesis.

2.2: Particulate Matter Exposure and Kidney Damage

Focusing on particulate matter (PM) exposure, growing evidence has demonstrated that chronic kidney disease (CKD) can be associated with ambient PM, thus supporting a potential mechanism for kidney damage [11-13,15-17,46-50]. Researchers focus on exposure to particles suspended, or resuspended, in the air with a diameter of less than 10 microns (i.e., PM10) and 2.5 microns (i.e., PM2.5). PM10 poses a concern as the particles can penetrate the airways within the lung. In contrast, PM2.5 particles can penetrate deep into the alveoli, where gas exchange occurs, potentially allowing translocation into the bloodstream. Bowe et al. (2017) and Lin et al. (2018) each conducted extensive national prospective cohort studies and found associations between kidney disease (CKD) or end-stage-renal-disease (ESRD) and PM10 or PM2.5, respectively.[46,48] Specifically, Bowe and colleagues (2017) determined an increased risk of CKD and ESRD with increased concentrations of PM10 (Risk = 1.07, 95% CI = 1.05-1.08) [48]. Meanwhile, Lin et al. (2018) concluded similar results that support an increased risk of CKD with increased concentrations of PM2.5 (Risk = 1.74, 95% CI = 1.53-1.98) [46]. An important feature of these two studies is the inclusion of a negative control that did not result in associations with either CKD or ESRD [46,48]. For example, Bowe and colleagues used the negative control of ambient air sodium concentration, a chemical lacking an association with kidney outcome. They tested if ambient sodium concentration and kidney outcome were associated and determined no association between the two variables (HR = 1.00, 95% CI = 1.00-1.01) [48]. Chan and colleagues (2018) also conducted a large cohort study that included 100,629 non-CKD individuals followed for up to 13 years [49]. They concluded an increased hazard ratio (HR = 1.15, 95% CI = 1.05-1.26) was associated with PM2.5 and CKD [49]. Chan

et al. (2018) also concluded a significant concentration-response model [49]. For every 10 ug/m^3 increase in PM2.5 concentration, there was a 6% higher risk of developing CKD (HR: 1.06, 95% CI: 1.02-1.10) [49]. Recently, two separate systematic reviews with meta-analyses were conducted by Wu et al. (2020) and Liu et al. (2020), investigating the above-mentioned studies and other smaller studies that associate CKD with PM exposure.[13,50] Wu et al. (2020), after conducting their meta-analyses, determined that a pooled summary risk ratio for every ten ug/m^3 increase in PM2.5 concentration was 1.10 (95% CI: 1.00-1.21) and a risk ratio for PM10 of 1.10 (95% CI: 1.05-1.29) [13]. Liu et al. (2020) concluded that the pooled summary risk ratio for every 10 ug/m^3 increase in PM2.5 concentration was 1.09 (95% CI: 1.03-1.17), and a risk ratio for PM10 of 1.08 (95% CI: 1.04-1.11) [50]. Notably, both studies clarified that there was considerable heterogeneity amongst the respective studies included in their reviews due to study designs, methodology for exposure assessments etc. [13,50]. Despite this, most of the studies' authors support the hypothesis that the effects of ambient PM and kidney health should be a public health concern warranting further investigation [13,46,48-50].

While there is little question regarding ambient air pollution’s effect on kidney health, researchers began investigating the impact occupational risk factors may have on kidney health. For example, the epidemics in Sri Lanka and Latin America appear to have a higher burden of disease in working populations. Sponholtz and colleagues (2015) conducted a case-control study investigating CKD-related occupational risk factors in North Carolina [15]. They concluded that industries experiencing “dusty” conditions have 2.19 times the odds (95% CI: 1.25-3.86) of glomerulonephritis than those working in non-dusty conditions [15]. Within these “dusty” industries, silica has been suggested as a major pollutant found within the dust [15]. Sponholtz and colleagues (2015) determined that silica exposure can be associated to farming activities and to CKD [15].

Perhaps more relevant to CKD and the overarching CKDu question, exposure studies have highlighted concern that workers in the sugarcane industry are exposed to high

concentrations of particulate matter [16,17]. One important consideration of sugarcane harvesting is the burning process, in which fields are purposefully burned to eliminate the excess plant on sugarcane. This increases harvesting efficiency for the sugarcane harvesters, often referred to as “cutters”, who enter the field and cut the sugarcane down. The cutters have been determined to be exposed to high levels of PM10 (~1800 ug/m^3) and PM2.5, containing silicate minerals and carbonaceous matter [14,17]. Considering the large effect of burning sugarcane fields and the generation of particulate matter, interest lies in the constituents of the PM present in the sugarcane fields. Le Blond et al. (2008) investigated what is contained within the burned plant matter, which predominantly comprises the sugarcane plant leaves [11]. They acquired several sugarcane plants and, in the lab, attempted to replicate the burning conducted in the fields prior to harvest [11]. The burned samples were then analyzed via Scanning Electron Microscopy (SEM) [11]. It was determined that prior to burning, most of the silica was in an amorphous state [11]. Post-burn, the majority of the silica present is released by the plant and, therefore, could not be determined to be in the amorphous or crystalline state [11]. Le Blond (2008) also concluded that during the burning process, some of the initial amorphous silica can be converted to cristobalite (one of the major polymorphs of crystalline silica) [11]. However, it is important to note that not all the silica was converted during the 3-minute or 10-minute burn times performed [11]. This suggests that most of the silica remains in its amorphous state and is also readily released into the air by the plant during the burning process. Leblond (2008) notes that the silica in the leaves is released as respirable-fraction (respirable = PM4 or smaller) [11]. Schaeffer and colleagues (2020) conducted a pilot-study on Guatemalan sugarcane cutters to characterize PM exposure [14]. The authors concluded that the composition of amorphous silica by weight on their samples was up to 17% [14]. Considering that the practice of burning the sugarcane fields is still prevalent across Latin America, exposure to PM is likely to remain high. The importance of understanding PM exposure in the context of silica on CKD, especially in the context of CKDu, can’t be understated.

2.2.1 Crystalline versus Amorphous

Given the different forms of silica and attendant health implications, an important differentiation between crystalline silica and amorphous silica is required. From a regulatory standpoint, while crystalline silica is carcinogenic and heavily regulated, amorphous silica has been classified by the International Agency for Research on Cancer (IARC) as “Not classifiable as to its carcinogenicity” [18]. It is important to note that the classification was based on lack of toxicological and epidemiological information. Further, an important note is to delineate the difference between carcinogenicity and nephrotoxicity. Carcinogenicity refers to a substance’s ability to elicit changes in a cell's DNA, causing cancer. In contrast, nephrotoxicity refers to the ability of a substance to damage the cells of the kidneys and may not cause cancer [19]. Further, many of the cited studies by IARC were conducted nearly 60-70 years ago [19]. As such, questions remain about exposure-response relationships related to amorphous silica, especially its potential to cause damage to the kidneys of these sugarcane workers. From a structural standpoint, the two major classifications of silica are crystalline and amorphous silicas. Structurally, crystalline silica contains a crystal lattice of Silicon-Oxygen bonding, while amorphous silica has an irregular Silicon-Oxygen bonding pattern (Appendix A) [18,19]. The primary subtypes of crystalline silica are alpha-quartz, tridymite, and cristobalite, with alpha-quartz being the most thermodynamically favorable of the group [18,19]. Amorphous silica is typically broken into synthetic and diatomaceous earth [19]. Diatomaceous earth is the geological derivative of algo, diatoms [18]. Differences in the structure between crystalline and amorphous lead to differences in analyzing the two chemicals. Crystalline silica is typically analyzed via X-ray diffraction following the National Institute of Occupational Safety and Health (NIOSH) Manual of Analytical Methods 7500 [23-25,28]. Amorphous silica, meanwhile, doesn’t

diffract X-ray, resulting in the process of calcining the amorphous silica to convert it to crystalline silica and then conducting NMAM 7501 [18,26].

In late 2023, studies emerged suggesting that amorphous silica exposure in sugarcane cutters may be via the nanoparticle size fraction (i.e., particles less than 1 micron in size) [20,21]. It is important to note that nanoparticles typically have characteristics that vary from the larger than 1 micron size fraction. Stem and colleagues (2023) published a study that concluded that exposure to sugarcane ash and derivatives disrupts the activity of mitochondria in proximal convoluted tubule cells and metabolomic activity in the proximal convoluted tubules [20]. This is supported by a previous study conducted by Sasai et al. (2022), who administered amorphous silica nanoparticles to Wistar rats via the lung and observed two key observations [21]. The first observation was that inhaled nanoparticles were of comparable size to sugarcane-sized ash, which was collected in studies where nanoparticles were isolated from the ash and resulted in kidney injury in the rats [21]. The second observation was that histologically, the damage observed in the kidneys of amorphous silica nanoparticle-exposed rats closely resembled the histological features of CKDu patients [21]. Another article unrelated to sugarcane cutters determined a potential mechanism for amorphous silica nanoparticles and kidney damage. The authors concluded that after exposing amorphous silica nanoparticles, which generally were considered inert, to thiol-containing biomolecules (such as glutathione), the thiols were oxidized, forming disulfide bonds [20,51]. In the Convoluted Tubule, glutathione helps to reduce free radicals present in the body, and as the glutathione is oxidized, the number of free radicals may increase [51]. Considering the novelty of these nanoparticles and how little research has been conducted on them, further research needs to be undertaken to determine the actual contribution of amorphous silica nanoparticles to health in general, especially in terms of kidney health.

In 2016, Bowe and colleagues conducted a global quantitation of CKD to PM2.5 exposure and concluded that Mesoamerican countries specifically suffer from significantly

higher CKD disability-adjusted life-year rates compared to other countries [12]. For reference, individuals living in Guatemala had a DALY rate of 408.4 per 100,000 (95% CI: 283.82-551.84) while individuals in Sweden had a DALY rate of 6.46 (95% CI: 0.00-14.49) [12]. In other words, Mesoamerican countries experience higher rates of life lost and years living with disability associated with CKD attributed to PM2.5 exposure. The importance of understanding the chemical constituents of particulate matter, especially with respect to the respirable fraction and amorphous silica's potentially deleterious role based on recently published studies and crystalline silica's nephrotoxicity, is a crucial next step in understanding CKDu.

2.3: Development of Infrared Spectroscopy for Crystalline Silica and Application for Amorphous

The gold standard for quantitating crystalline silica analysis is X-Ray Diffraction (XRD), which is widely used by the United States Occupational Safety and Health Organization (OSHA) for its regulatory silica limits (i.e., NMAM 7500 and NMAM 7501) and used by the National Institute for Occupational Safety and Health Organization [23-25]. Recently, silica analysis has undergone several advancements.

In 2016, the United States OSHA decreased the Permissible Exposure Limit (PEL) from 250 ug/m^3 to 50 ug/m^3 for respirable crystalline silica, a 20% reduction in allowable exposure in the workplace [23]. This arose because the outcome of crystalline silica exposure, silicosis, is a deadly but preventable disease [22-24]. The decreased PEL created an increased need to analyze samples to ensure compliance rapidly and accurately. The primary concern with XRD is the time-consuming nature of the analysis, which requires multiple laboratory preparation steps.[25,26] The result is, at minimum, a potential one-to-two-week delay between sampling the worker and receiving the results of that sample, meaning that the worker could potentially be overexposed for multiple work shifts before controls are implemented [27,29,52]. Additionally, the cost of analysis via XRD is a considerable concern, especially for companies working in high-silica exposure industries. Prices range depending on the laboratory conducting the

analysis but typically fall in the $180-300 price range per sample. For a company that may need to conduct samples weekly on multiple employees, the cost will increase considerably with the addition of a one-to-two-week delay in results. The alternative/complementary method to XRD that is currently in use in the United States is using Fourier-Transformed-Infrared Spectroscopy (FTIR) [28]. This method requires the destruction of the filter and deposition into a Potassium-Bromide pellet before scanning for silica peaks [28]. In this analytical technique, while the overall cost is lower, the laboratory preparation of the sample also creates a delay between the day sampled and the day the results are received [28,29]. An important note needs to be made that both analytical techniques cannot determine crystalline silica results on the same day as sampling. Further, both methods require the filter's destruction, meaning that further analyses can't be conducted. Amorphous silica suffers significant laboratory concerns as the amorphous nature of the analyte means direct XRD is impossible [19,26]. A lengthy preparation requiring redeposition onto two separate filters before the concentration can be determined is needed to accomplish quantitation [26]. To summarize, the filter is ashed and redeposited onto a new PVC filter and subsequently analyzed for each polymorph (i.e., alpha-quartz, tridymite, cristobalite) as a baseline scan. The filter is then ashed in a crucible at 1100 °C for six hours. The ash is then transferred and ground into a fine powder before being redeposited onto a silver filter and analyzed again for the polymorphs mentioned above. The increase in cristobalite concentrations at baseline versus post-calcined gives the concentration of amorphous silica present [26]. Consequently, this analysis results in a destructive technique requiring a one-to-two-week delay and a very costly analysis that can approach double the cost of analyzing crystalline silica. While these analytical techniques are accurate, their shortcoming is in the time required to conduct the analysis, the destructive nature of the techniques, and the potential cost per sample placed on the company or the research laboratory interested in determining the concentration of the analyte.

Due to the recent regulation changes in crystalline silica PELs (i.e., OSHA Silica PELs in 2016 and MSHA Silica PELs in 2024) and the increased request for faster analytical techniques that are comparably accurate, recent emphasis has been placed on real-time monitoring/end-of-shift analysis or direct-on-filter, non-destructive techniques [27,29,52]. This results in accurate analytical results faster for various analytes of interest in the industry while reducing cost. With these challenges in mind, NIOSH and colleagues have been developing and optimizing Fourier Transformed Infrared Spectroscopy (FTIR) analytical techniques [27,29,52].

The method involves taking a filter collected during a sampling campaign, inserting the filter into the device, and scanning the filter with infrared light to determine which particles were deposited onto the filter. As each chemical absorbs the infrared light at a specific wavelength of light (cm^{-1}), the infrared light can be used to quantify the mass of silica present using specialized computer software [27,29,52]. The software, “Field Analysis of Silica Tool” (FAST), uses a pre-constructed model and applies the model to each filter’s absorbance spectrum to predict the concentration of crystalline silica on a filter.

Samples are analyzed with the infrared spectrometer to determine the strength of absorbance by crystalline silica to generate the model. Then, the filter is sent to a lab to be analyzed by XRD to quantify the crystalline silica present on the filter [27,29,52]. With the known concentration determined by XRD and the absorbance value determined by the FTIR, the two variables can be plotted against each other in the FAST software [27,29,52]. The model can then predict unknown crystalline silica concentrations based on the FTIR's absorbance value [27,29,52].

After the FAST software was released, NIOSH continued to conduct studies on the FAST’s accuracy and application outside of the mining field [27,29,52]. In a study comparing the FAST software to XRD, the authors determined that the FTIR quantitation fell within 10% of XRD quantitation values at three separate mine sites. The FTIR quantitation typically underestimates RCS concentrations relative to XRD [52]. Hart and colleagues (2018) concluded

in their study that the FTIR method is a possible alternative analytical method to quantify respirable crystalline silica values comparable to the same sample analyzed via XRD [52]. Further, they conclude at the end of the study that FTIR could be applicable to non-mining environments [52]. NIOSH also suggests that their FAST software may be applicable to quantitate crystalline silica in environments that are not coalmines, but the results will be approximations [52]. From these developments by NIOSH, it can be concluded that faster and comparable methods to analyze crystalline silica are possible using FTIR software with partial-least square regression to adjust the quantification model.

Interfering minerals in the samples pose a limitation in the studies conducted by Hart, Cauda, and others using FTIR. In coal mine settings, this is typically kaolinite [27,29,52, 53]. Outside of the mine setting, the interference of silicate materials such as amorphous silica, the analyte of interest of this project, is a serious concern to the FTIR FAST Software since the polymorphs of silica (i.e., quartz, cristobalite, amorphous silica), have similar wavelengths to each other [27,29,52,53]. According to Ojima, (2003) amorphous silica was generally considered a non-interfering mineral to crystalline silica determination [53]. However, the peak at 800 $cm^{-1,}$ commonly used for RCS determination, can suffer interference from amorphous silica since it also peaks at 800 cm^{-1} [53]. Ojima also mentions several wavelengths that amorphous silica can interfere with crystalline silica, all of which can be used in crystalline silica determination [53].

It should be noted, therefore, that XRD is essential in these studies to confirm the presence of crystalline silica. However, it is equally important to determine that interference minerals are not present as they can potentially cause an overestimation of the FTIR model if not corrected [53]. The FTIR method, while having these limitations, can overcome them if accurate analysis is conducted and the determination of interference mineral presence is confirmed.

In conclusion, the FTIR method should be coupled with XRD analysis due to the various polymorphs to ensure the model can be applied accurately [27,29,52]. To apply the FTIR method discussed above to amorphous silica, some steps for the crystalline silica FTIR method should be adjusted. XRD quantitation should be used to confirm the lack of crystalline silica to reduce the risk of interference as mentioned above. As discussed here, the analytical techniques of amorphous silica are limited due to the general consideration that amorphous silica is not classifiable as harmful to human health [18]. Given that CKD in Mesoamerica and other locations across the globe currently has an unknown set of risk factors contributing to its incidence, attempts to quantify amorphous silica to confirm or eliminate its potential contribution should be conducted.

3. METHODS

3.1 Air Sampling & Gravimetric Analysis

A pilot study was conducted as a proof of concept for developing direct on-filter analysis of amorphous silica using FTIR. Briefly, personal air samples were collected in December of 2021 near Santa Lucía, Cotzumalguapa, in Southwestern Guatemala. The respirable fraction was collected using Parallel Particle Impactor (PPI) samplers (SKC Inc., Eighty-Four, PA, USA) loaded with 37-mm poly-vinyl chloride filters (pore size of 5.0 μm) and attached to SKC AirChek XR5000 (SKC Inc, Eighty-Four, PA, USA) sampling pumps. Each PPI sampling train was pre- and post-calibrated to 2 liters per minute (L/min) using a primary flow standard. Samplers were placed in the breathing zone of sugarcane workers who performed tasks such as cutting and stacking sugarcane into rows [14].

Following the pilot study, subsequent field campaigns employed a new sampling strategy using 37-mm SKC Aluminum Respirable dust cyclones (SKC Inc, Eighty-Four, PA, USA) with SKC AirChek XR5000 (SKC Inc, Eighty-Four, PA, USA) pumps. The cyclones were loaded with the same filter media described above, and the sampling trains were pre- and post-calibrated to 2 L/min, which shifted the 50% cut-point to 5 μm in size.

Samples were transported back to Colorado State University for gravimetric analysis per a standard operating procedure [14]. Filters were desiccated for 24 hours and then static neutralized with a U-Electrode (Mettler-Toledo, Inc.) before post-weights were collected. The mass of each filter was conducted on a Mettler MT5 balance (Mettler-Toledo Inc. Columbus, OH, USA).

3.2 Infrared Spectroscopy Measurements

Samples were analyzed using an FTIR spectrometer (PerkinElmer Spectrum Two, Waltham, MA, USA). A Sedulitas (Sedulitas Company, Potchefstroom, South Africa) 37-mm

sample holder was used to align the center of each filter in the beam path of the spectrometer. Transmission spectroscopy was chosen over attenuated-total-reflection (ATR) spectroscopy because ATR requires contact with the sampled area. In contrast, transmission only involves the edge of the filter being in contact with the holder, thus preserving the non-destructive nature of the aim of the study. The FTIR was programmed to analyze each filter at a resolution of 4 $cm^{-1,}$ and 16-32 scans were collected and averaged for each filter to minimize noise.

PerkinElmer Spectrum IR Software (PerkinElmer, Waltham MA, USA) was then used to plot all infrared data and allow for visual confirmation of silica peaks. In infrared spectroscopy, peaks refer to sharp increases in the infrared light absorbed by a molecular bond, removing that infrared light from the detector's path. Specific elemental bonds exist at different regions of the infrared spectrum and can be used for the identification of molecules. For example, the silicon dioxide bond typically absorbs infrared light at 1094 and 800 $cm^{-1,}$ amongst other wavelengths. Filters were then sent to confirm amorphous silica presence and for crystalline silica measurements via XRD and NMAM 7500.

3.3 XRD Analysis

After samples were analyzed using the infrared spectrometer, a subset of filters were sent to EMSL Analytical (EMSL Analytical Inc., Cinnaminson, NJ, USA) for analysis of crystalline silica and amorphous silica, following NMAM 7500 and NMAM 7501, respectively. Due to the NIOSH Manual of Analytical Methods (NMAM) 7500 for crystalline silica and 7501 for amorphous silica requiring different preparation techniques, samples were cut in half. Future cyclone samples would only need to be analyzed for amorphous silica and would not require cutting the filter in half.

3.4 Development of Predictive Model

Once XRD results were received, confirmation of amorphous silica allowed the model to be constructed. Using PerkinElmer Quant Spectrum Software (PerkinElmer, Waltham MA), areas under selected peaks were calculated and then correlated against the known value of amorphous silica, creating a correlation plot. The software also allowed for Principal Component loads to be conducted to determine which corresponding wavelength creates the greatest variation in absorbance to determine if the peak at 800 cm^{-1} was also viable for amorphous silica.

3.5 Development of Filters with Known Amounts of Amorphous Silica

To determine the amount of uncertainty or inconsistency in analyzing for amorphous silica, filters needed to be loaded with only amorphous silica. An aerosol sampling chamber was used (Appendix B). The Aerosol sampling chamber had 3 inlet/outlet points: 1.) air inlet valve where air was pumped into the chamber to both generate dust and compensate for the loss of air through the filter 2.) An air outlet for the DustTrak DRX Aerosol Monitor (TSI Instruments Inc. Shoreview, MN, USA) 3.) A second air outlet allowed the tubing from the SKC AirChek XR5000 (SKC Inc, Eighty-Four, PA, USA) to connect to the sampling train. Two size fractions were collected using two different samplers in this loading project. The first sampling train was connected to a BGI Cyclone (MesaLabs Inc., Lakewood, CO, USA) were loaded with a 37-mm Polyvinyl Chloride filter with a 5-micron pore size (SKC Inc. Eighty-Four, PA, USA). The sampling train was programmed to run at a rate of four liters per minute to collect a size fraction of 2.5 microns. The second sampling train used an SKC Aluminum Cyclone (SKC Inc. Eighty-Four, PA, USA) loaded with a 37-mm Polyvinyl Chloride filter with a 5-micron pore size. The SKC cyclone sampling train was set to run at a rate of two liters per minute to collect a size fraction of 5 microns. Sampling duration occurred for either 240, 120, or 60 minutes. Diatomaceous Earth, also known as amorphous silica (Woodstream Inc, Lancaster, PA, USA),

was placed into the aerosol chamber. The starting amount was approximately 10 milligrams. The BGI Cyclone was then suspended inside the chamber (Appendix B). After sealing the chamber and attaching the AirChek pump, house air at approximately 10 liters per minute was supplied into the bucket to suspend and disperse the amorphous silica in the chamber. Using the DustTrak, ambient air concentration within the aerosol chamber typically approached 2.0-3.0 mg/m^3 while the sampler operated. The house air was set to match the pump's flow rate using a rotameter to keep the system in equilibrium (4 liters per minute for PM2.5 or 2 liters per minute for PM5). After the sampling, filters were desiccated for 24 hours before conducting FTIR and gravimetric analyses. Conducting gravimetric analysis pre- and post-sampling and controlling the aerosol chamber to allow only amorphous silica deposition meant that any mass gain on the filter must be due to amorphous silica depositing on the filter.

4. RESULTS AND DISCUSSION

4.1 Initial Proof-of-Concept and Feasibility of DOF FTIR Methods for Amorphous Silica

The pilot study analyzed 99 PPI samples with a median mass of 190 µg. The minimum mass gain was 0 µg, while the maximum mass gain was 2057 µg. After the filters were scanned and entered the PerkinElmer Spectrum IR software, the spectrum of each filter (Fig. 1a) was compared to a reference spectrum of amorphous silica acquired from the PerkinElmer Spectrum IR software database of chemicals. Amorphous silica has peak absorbances of Silicon-Oxygen bonding at 800 cm^{-1} and 1094 cm^{-1} [53]. As discussed in Ojima et al. 1994, crystalline silica also has known peak absorbances in this region, resulting in concern about the co-occurrence of crystalline silica given its prevalence [53]. This argument is valid in environments where sources of crystalline silica are present. However, Leblonde and colleagues determined that sugarcane particulate matter released during burning events was dominantly amorphous silica present in the leaf, and it often failed to be converted to crystalline silica either due to insufficient temperatures (>1100°C) or burn time (>10 min) [11].

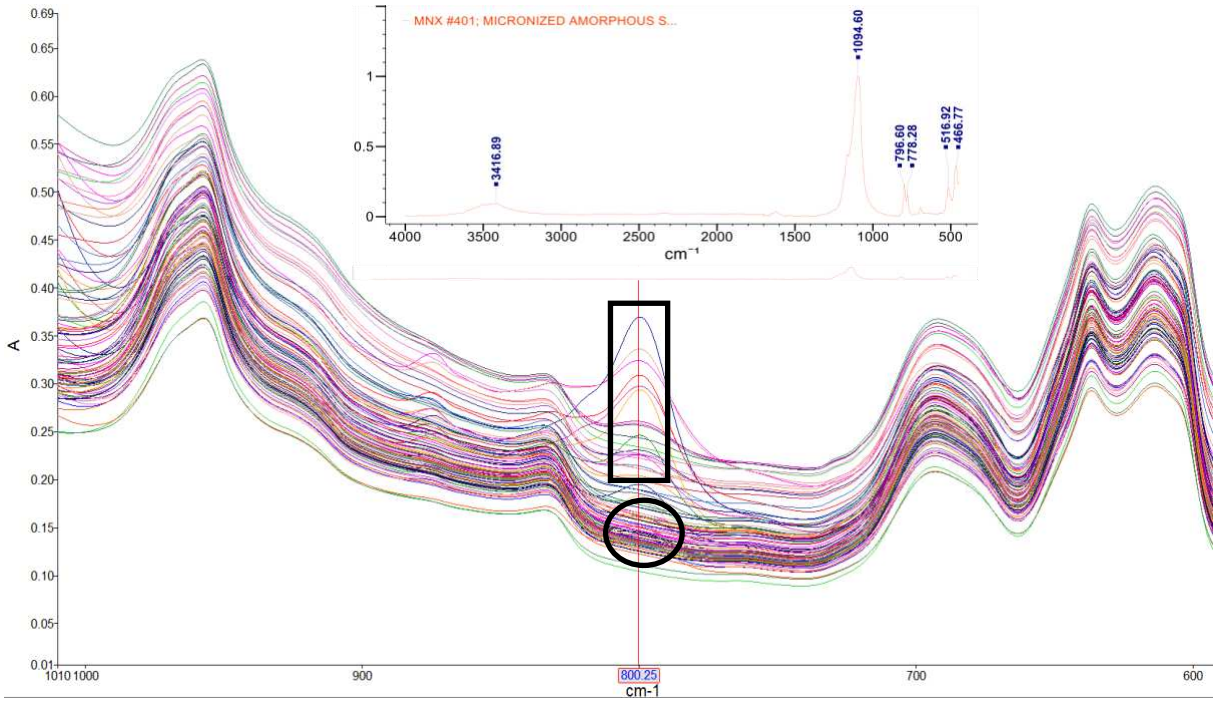

Figure 1: A zoomed-in infrared spectrum of PPI samples. Peaks highlighted in the black rectangle (i.e., at 800 cm^{-1}) indicate amorphous silica. In contrast, spectra highlighted in the black circle represent field-blank samples with little to no amorphous silica present. The full spectrum of micronized amorphous silica is depicted in the insert to show representative spectra.

Comparing the sample and reference spectra in Figure 1, only 11 filters presented with a peak at the 800 cm^{-1} wavelengths, while the remaining 84 filters did not exhibit this characteristic absorbance. In other words, the 84 samples all display a spectrum that matched the spectrum observed in a field blank, suggesting insufficient deposition for the FTIR to detect. A subset of these 11 “positive” amorphous silica samples were then sent to EMSL for amorphous silica quantitation via XRD (Table 1) to build a model to analyze and predict the mass of amorphous silica present in the cyclone filters non-destructively.

Table 1: X-Ray Diffraction Determined Masses of Amorphous Silica on PPI Filters

Sample ID	Amorphous Silica Mass (mg)
PPI001	<0.005*
PPI006	0.007*
PPI010	<0.005*
PPI014	0.038*
PPI019	0.051*
PPI027	0.005*
PPI042	0.009
PPI044	0.042
PPI049	0.011
PPI066	0.008
PPI073	<0.005

*- denotes these filters were analyzed as half samples due to the limitation of NMAM 7501 and 7500 compatibility.

To better understand the variabilities between each filter and what is driving the variability, a principal component analysis (PCA) was conducted. The PerkinElmer software generated a plot based on the variability of the wavelengths between each filter (Figure 2a). From Figure 2a, one variable (or wavelength) accounted for 96% of the variability between filters. Additionally, it can be noted that the rest of the spectrum only accounts for 4% of the variability suggesting that the filters remain relatively constant. A principal component plot was generated to determine which component had the greatest variability (Figure 2b). As such, the peak at 800 cm-^{1} had the greatest variability as well as at 1090 cm^{-1} and approximately 1250 cm-^{1} (Figure 2b).

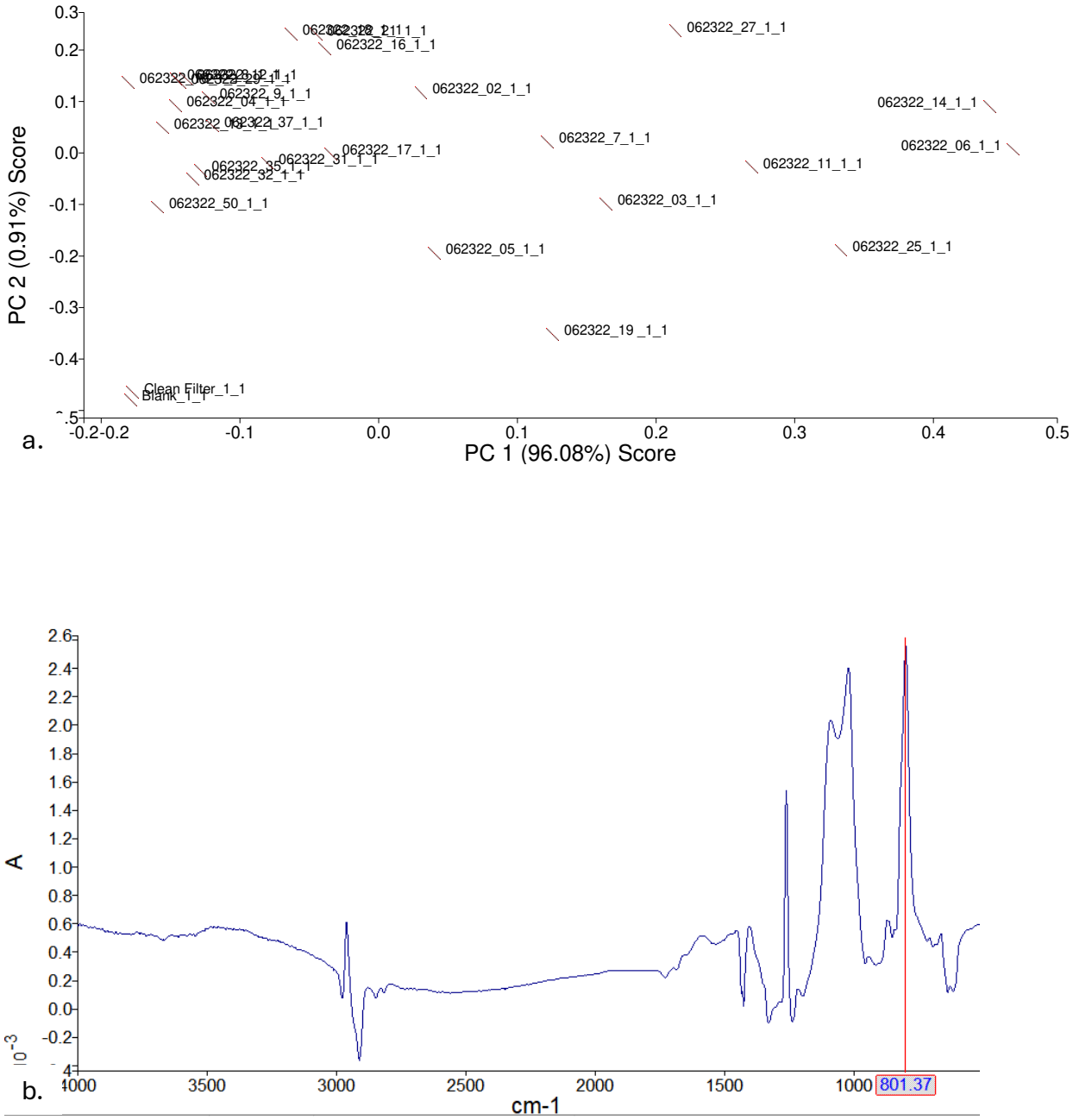

Figure 2: Correlation spectra graphs: (a) Principal Component Analysis of 25 PPI samples with two blank filters. Each filter is plotted on the graph based on the variability of the wavelengths between itself and the previous and subsequent samples. The wavelength with the greatest variability will be labeled on the x-axis as principal component 1, while principal component two is the second greatest variability between the filters; (b) A plot of the wavelengths with the highest deviation. Peaks with increased absorbance indicate high variability at the respective wavelength amongst each filter. Troughs are generally ignored in correlation spectra.

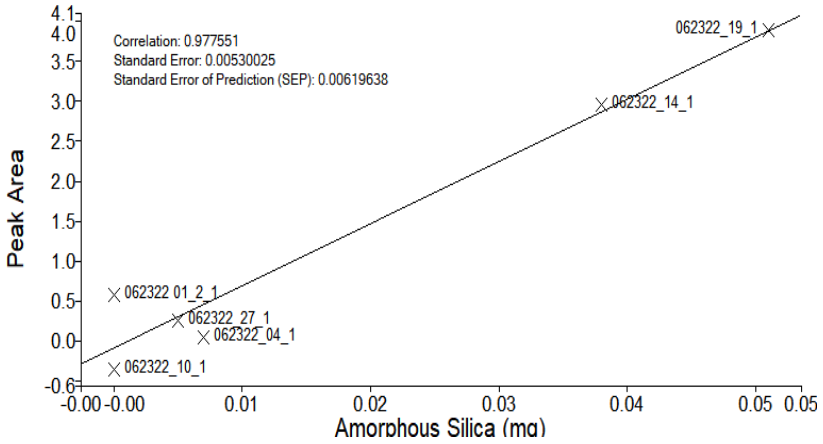

Figure 3: Correlation plot of known concentration of amorphous silica vs. peak area. The correlation plot relates the mass of amorphous silica vs. the area underneath the silica absorbance peak at 800 cm^{-1}. This is the model that allows the software to take a filter with an unknown mass, scan it with infrared light, and then based on the peak area absorbance, predict the mass present on the filter. The correlation of 0.978 suggests that the two variables are strongly positively correlated.

After scanning the PPI filters with the FTIR, samples that tested positive with amorphous silica were then plotted in Spectrum Quant (PerkinElmer, Waltham MA). The known mass of amorphous silica (previously determined via XRD in Table 1) was plotted against the area underneath the 800 cm^{-1} peak as seen in Figure 3 . These results were indicative of a strong linear correlation with an R^2 value of 0.978 meaning that as there is an increase in the absorbance detected by the FTIR, there is a corresponding increase in the mass of amorphous silica present on the filter.

From these results, the procedure for analyzing amorphous silica worked and the model could be created. The next step was therefore to apply the model to new samples and determine the accuracy of the model in predicting the mass of amorphous silica present.

4.2 Application of Pilot Model to Cyclone Filters

Based on the proof of concept and the constructed model, the next step was to apply the correlation plot curve (Figure 3) to the cyclone filters collected from sugarcane cutters. Each filter was by scanned, allowing the model to estimate the mass of amorphous silica based on the absorbance detected. An important aspect of this model that was the requirement of a peak at a wavelength of 800 cm^{-1}, which indicates the presence of amorphous silica. From the six sampling campaigns conducted between December 2022 and April 2023, 109 personal cyclone samples were analyzed by FTIR (Figure 5). The median mass collected on the 109 cyclone filters was 188 µg with a minimum mass of 14 µg and a maximum of 975 µg.

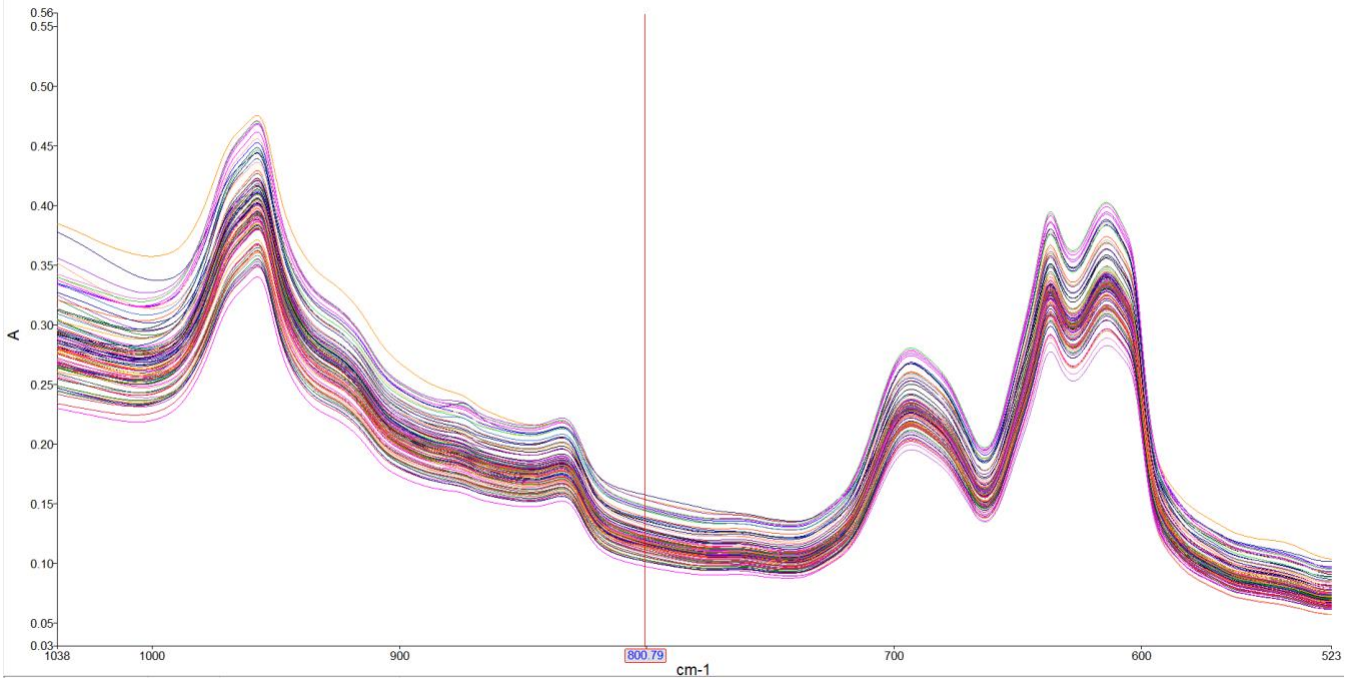

Figure 4: Cyclone Samplers acquired from Sugarcane Cutters in Guatemala showing the wavelength of interest at 800 cm^{-1}.

As can be seen in Figure 4, the cyclone data do not contain a peak at 800 cm^{-1}. Instead, the data present a flat area ranging from 750-850 cm^{-1}. Consequently, there was either no amorphous silica present in these filters, or the amount of amorphous silica could not be determined using this method of the FTIR. According to Cauda and colleagues in their FTIR studies for the limit of detection of crystalline silica, the limit of detection is approximately 5 µg while the limit of quantification is 16 µg [27]. Therefore, if the latter of the two potential issues were occurring, then there would be a higher uncertainty not accounted for to analyze for amorphous silica than for crystalline silica. Several cyclone field blanks were also included in the model and the attendant spectra were nearly identical to the samples collected from the sugarcane workers. This suggests no difference in the composition of elemental bonding between the samples collected in the field and the field blank samples.

4.3 Lab Loading Project

Due to the null results of applying the FTIR model to the cyclone samples collected from the breathing zone of study participants, this final project aimed to evaluate spectral differences in sample type (i.e., PM5 versus PM2.5) while using an aerosol chamber to load amorphous silica. In this study, two separate experiments were conducted to provide better insight into the detection of amorphous silica using FTIR. The significant difference between the experiments was the size fraction. Study 1 investigated a size fraction of $PM_{2.5}$, versus the second study that used a size fraction of PM_5. This was done to determine if there is an effect on the results of the FTIR when using different samplers and sampling PM sizes.

The first study collected diatomaceous earth at a 2.5-micron size fraction using the BGI Cyclones. 44 samples were collected with a minimum loading of 15 $\mu g/m^3$, a median of 192 $\mu g/m^3$ and a maximum of 5100 $\mu g/m^3$. Since the sampling chamber only contained diatomaceous earth (amorphous silica), any mass increase on the filter must be attributed to amorphous silica loading. The range of the samples was wide primarily due to the unpredictable

nature of loading the amorphous silica onto the filters. For example, in the same sampling session one filter may be loaded with 50 micrograms of amorphous silica while the next filter was loaded with 250 micrograms of amorphous silica.

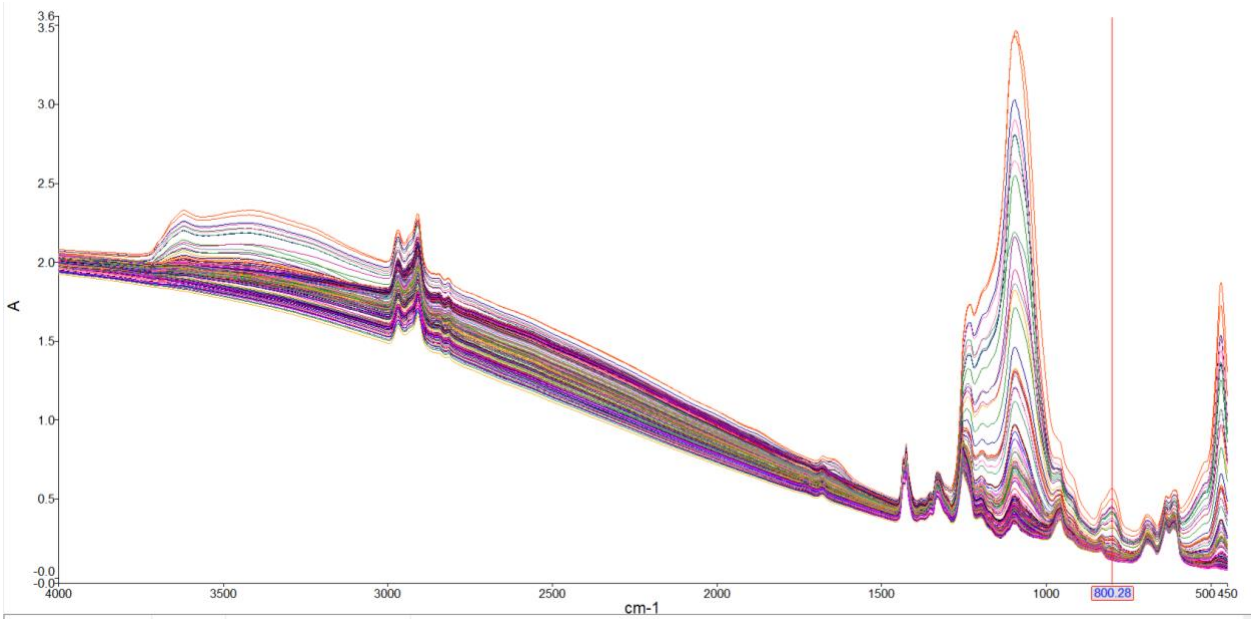

Figure 5: FTIR spectra for filters (n=44) that were loaded with diatomaceous earth. Peaks occur roughly at 1094 cm^{-1} and 800 cm^{-1}.

Considering the strong positive correlation from the pilot study, collecting a wide range of samples allows for the determination of when the FTIR is no longer able to detect the peak, giving an estimate of the limit of detection for the pilot model. A principal component loading plot was built (Figure 6) to determine the wavelengths with the greatest variability and confirm that the spectra matched the amorphous silica reference spectrum (Figure 1). The wavelengths at 1094 and 800 cm^{-1} are the wavelengths with the greatest variability and support that the filters were loaded with amorphous silica. Additionally, as can be seen in Figure 3 with the PPI samplers, the two correlation plots have similar absorbance bands with variability, suggesting that Si-O bonding is occurring in both sets of samples.

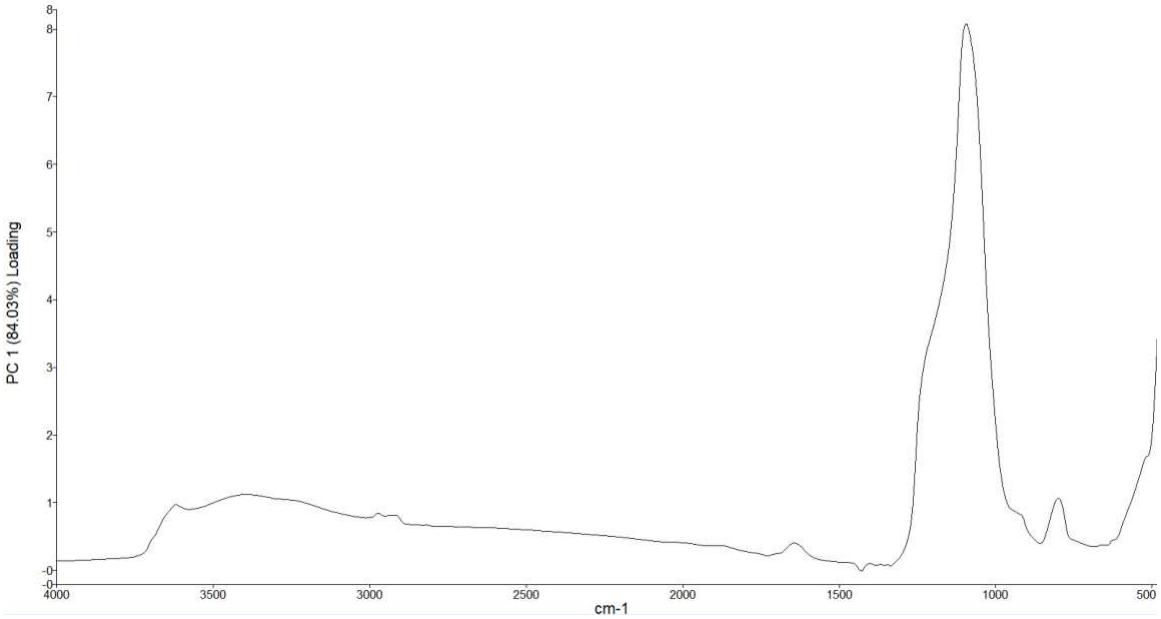

Figure 6: Principal Component Loading Plot

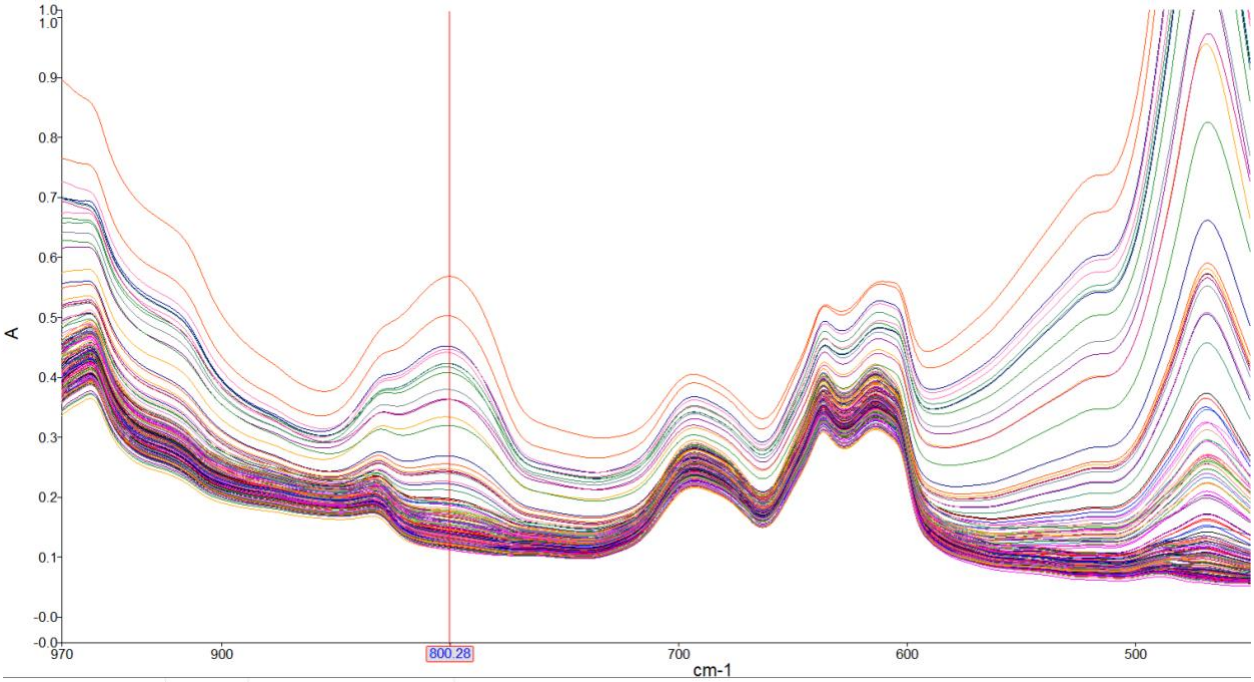

Figure 7: Zoomed in view of the amorphous silica loading experiment with a focus on800 cm^{-1} where the silicon dioxide bond is expected to be present.

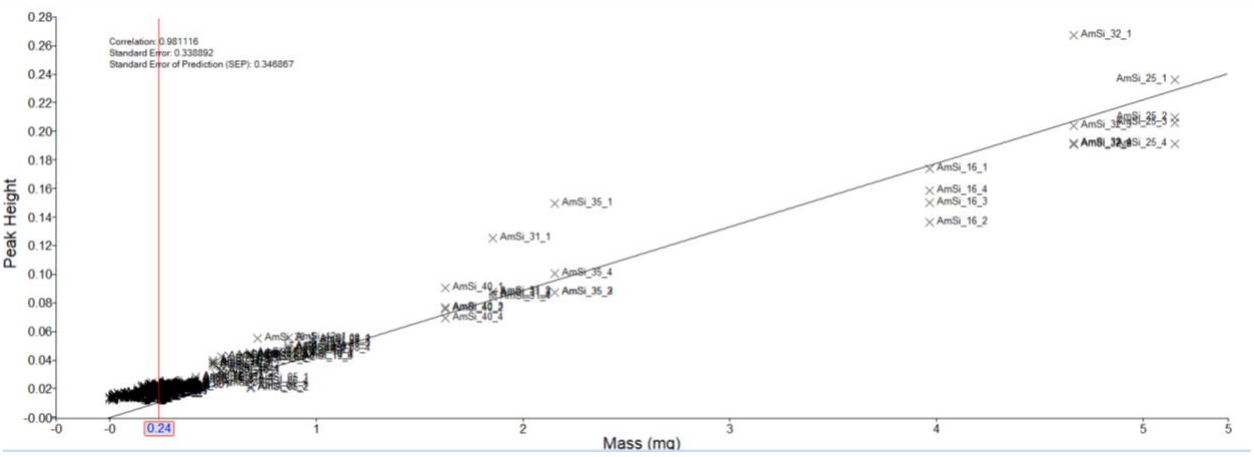

Figure 8: Correlation plot relating known concentration of amorphous silica to peak height intensity at 800 cm^{-1}. The line of best fit was used to estimate the mass of amorphous silica present on a filter based on the peak height intensity.

As shown in Figure 8, a strong correlation of 0.98 was observed. This was observed in Figure 7, where the peak at 800 cm^{-1} slowly decreased in terms of max peak height and, in turn, peak area until the band approached a spectra appearance like the field blanks. At approximately 500 micrograms, the peak intensity at 800 cm^{-1} was inconsistent with the mass loaded on the filter vs. the absorbance reading produced. For example, some of the samples contained greater than 500 micrograms on the filter, yet the absorbance at 800 cm^{-1} approaches 0 units; meanwhile, a different filter with 400 micrograms of amorphous silica displayed a stronger peak. This likely represents an approach towards some uncertainty of analyzing amorphous silica with the instrument. This could be due to amorphous silica's amorphous nature as demonstrated earlier. Without a definitive crystalline structure, some of the amorphous silica may not absorb as well as others.

However, given that these samples were collected at a smaller size fraction, an additional set of samples were collected in the aerosol chamber (n=20) following the SKC cyclone method of PM_5. The sampling campaign for 5-micron particulate using an SKC aluminum cyclone resulted in a median mass of 857 micrograms, a minimum of 220 micrograms, and a maximum of 5.3 milligrams. Figure 9 depicts the spectra of the PM_5 samples where approximately five peaks are qualitatively present, while the remaining 15 have a smaller peak in the range of only 0.05 to 0.1 absorbance units in height. This would suggest that these 15 samples would have lower amounts of diatomaceous earth present on them, however, given a median mass (857 µg) well above 500 micrograms, there should be an increased number of tall peaks. This likely is indicative of an inconsistency with the FTIR in scanning filters that may be due to uneven filter loading causing the beam path to miss the diatomaceous earth. Additionally, this inconsistency seems to suggest that the larger size fraction has a higher limit since the inconsistency starts at a mass closer to 800 microns near the median mass of the 20 samples.

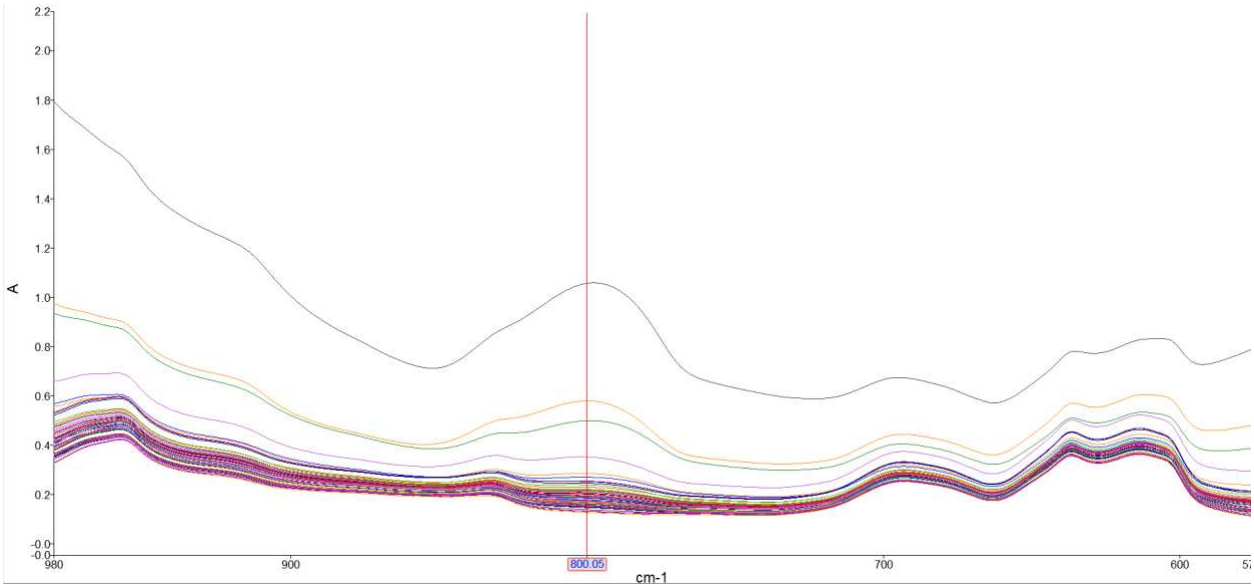

Figure 9: IR spectra of samples (n=20) acquired using an SKC Aluminum Cyclone to collect 5-micron particulate.

Interestingly, when these data were analyzed using the model generated in Figure 8, the model predicted values for this increased size fraction data. Within the 20 samples, the model had an average residual value of -0.413, suggesting it typically overestimates the predicted value. A moderately strong correlation between the predicted and known masses was observed. This likely suggests that the model and the FTIR can detect amorphous silica on PVC filters and potentially determine concentrations of increased and decreased amounts of amorphous silica (i.e., it can detect one gram of amorphous silica and differentiate that from one-half gram present). However, the uncertainty needs to be considered. Additionally, from the inconsistencies mentioned earlier, measured around 500 cm^{-1}, when the model predicts a value of 0 mg of amorphous silica deposited on the filter, the actual mass is 262 micrograms, suggesting that the model has uncertainty in accurately predicting masses near or below 262 micrograms. However, given the above concern about inconsistencies at 500 micrograms, this latter value should be used cautiously until further research is done to determine the cause of the discrepancies.

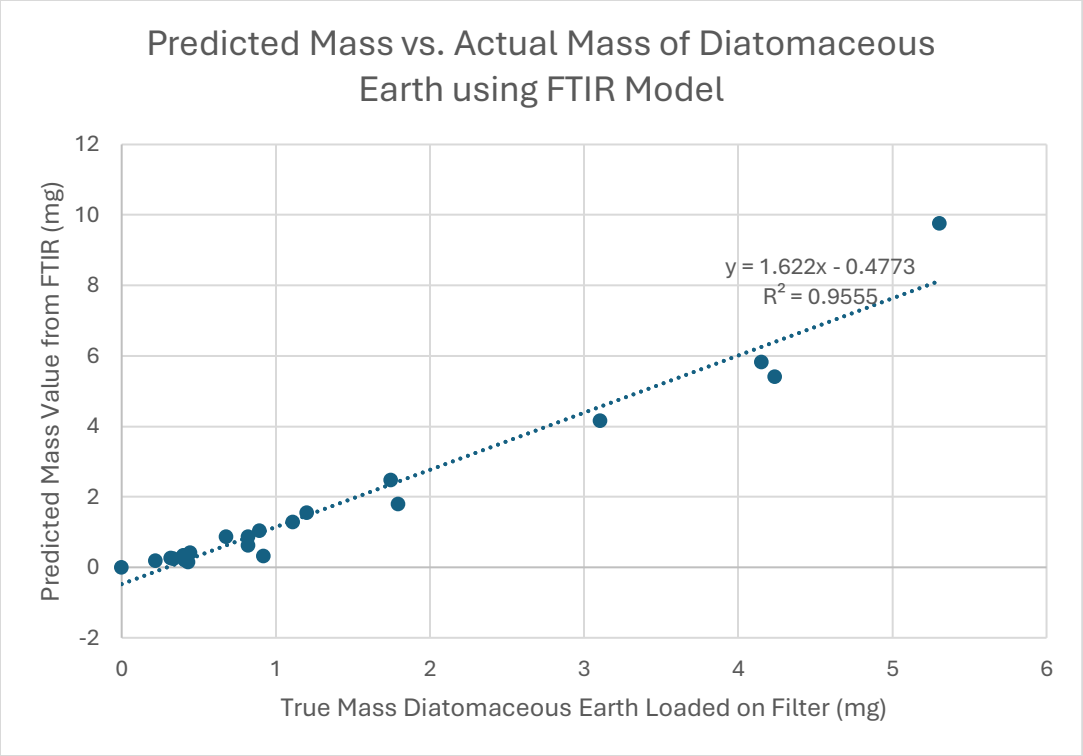

Figure 10: Plot of predicted mass using the model generated by FTIR in comparison to the actual mass gain of the filter using an increased size fraction (PM5)

4.4 Limitations and Observations

From these three applications of the FTIR, several observations were made. The first observation was that the PPI cyclones allowed amorphous silica particles to be detected using FTIR at levels lower than 100 micrograms of amorphous silica, which contradicted the results of the lab loading study. Several samples within the pilot study (i.e., 42, 44, 49, 66, and 73) tested positive for amorphous silica via XRD, yet didn't test positive for amorphous silica on FTIR (Table 1, Figure 11). For example, sample 19 contained approximately 51 micrograms of amorphous silica and displayed a peak at 800 cm^{-1}, while sample 44 contained 41 micrograms of amorphous silica and didn't display a peak at 800 cm^{-1}. This concern was also seen in the lab loading study with some of the samples collected, as mentioned above. The likely issue here is depositional differences on the filters, meaning the infrared light isn't hitting the correct area of

the filter, resulting in a null result despite the presence of amorphous silica. Further studies will look to find a cause for this issue, as it is present in multiple aspects of the study.

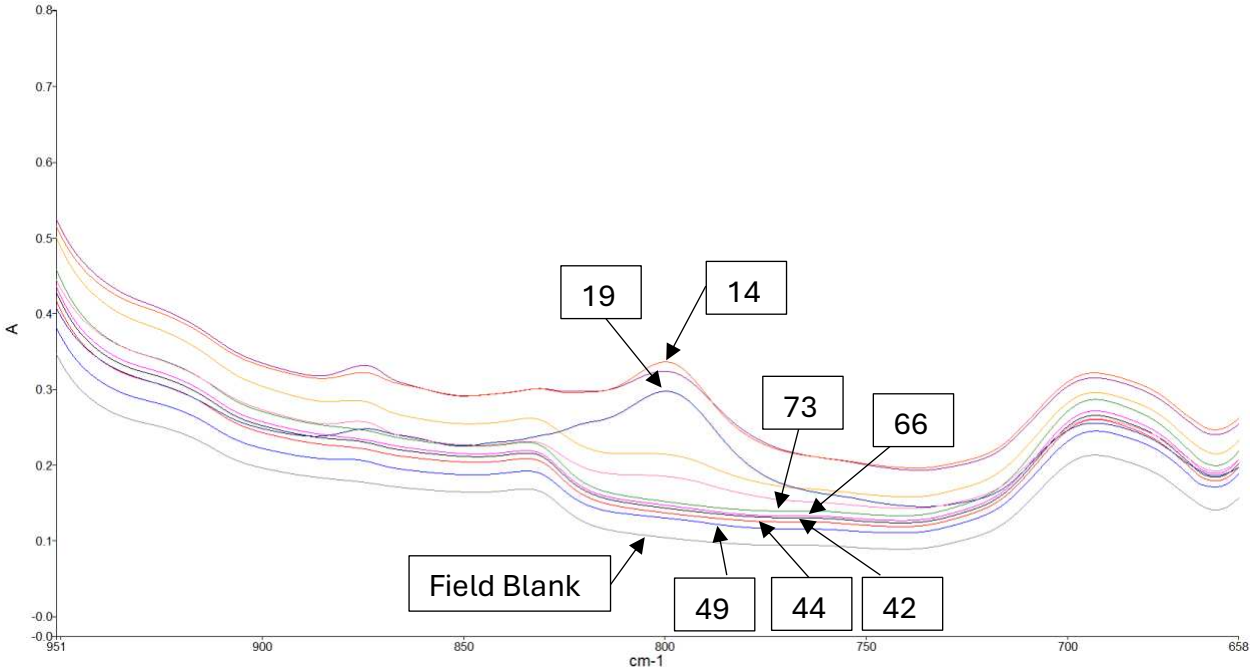

Figure 11: IR spectrum of PPI samplers (n=11) collected in Guatemala. Each arrow points to a specific line representing a sample. For reference, the arrow pointing to the lowest spectrum on the graph is the field blank, representing no increase in absorbance at 800 cm^{-1}.

After the model was created using these PPI pilot filters, there was a strong positive linear correlation between the absorbance generated with infrared spectroscopy and the mass of amorphous silica on the samples. When attempting to apply the model, which used a peak area calculation at a wavelength of 800 cm^{-1}, to more recent sampling campaigns that use an aluminum cyclone vs. a parallel particle impactor, an issue arose due to the cyclone samples lacking a peak that was representative of amorphous silica. Third, a lab loading project was attempted to understand where the FTIR instrument begins to attribute absorbance to the mass of amorphous silica incorrectly. It was determined that inconsistencies arose near 500 micrograms. Interestingly, this is nearly five times higher than the pilot project could detect.

One hypothesis regarding this contradiction is the theory that the PPI samplers were overloaded due to the high concentrations of PM entering the device, resulting in the sloughing off of larger than 10-micron particles onto the filter, causing the detector to detect these high-mass particles. This might also explain why aluminum cyclone filters do not have an amorphous signature. In other words, when transitioning to the cyclone, it is much harder to overload due to the large grit pot at the bottom of the cyclone to catch particles larger than the four-micron cut point. This could result in the loss of these large particles, impacting the filter and creating peaks on the FTIR.

There were several limitations within the project worth discussing. Firstly, research on amorphous silica is nearly nonexistent from an occupational exposure standpoint. As seen in the literature review, many researchers focus on crystalline silica and/or see amorphous silica as a confounder in their data when both are present. Secondly, infrared spectroscopy has only recently been widely used outside of the mine setting, meaning there are many unknowns and hurdles to fine-tuning the FTIR for open-exposure type direct-on-filter techniques such as this.[38,27,29] Thirdly, the lab loading project was conducted assuming there was no co-contamination of the diatomaceous earth with crystalline silica (the company marks the ingredients as trade secrets). This limit is relatively minor, however, given that crystalline silica is known to be detectable at levels approaching five micrograms in size and would undoubtedly have generated more substantial peaks at lower levels of deposition on the filters.

5. CONCLUSION

Chronic kidney disease of unknown origin is an epidemic that remains prevalent in agricultural communities around the globe. In Central America, sugarcane harvesters, also known as sugarcane cutters, are experiencing a high burden of the disease, which in its later stages requires medical care that is typically unavailable to the workers. It is, therefore, imperative to begin to understand the risk factors that may be contributing to the disease's burden. Several hypotheses have been proposed, especially concerning aerosol exposures to heavy metals or silica, many of which are potential nephrotoxins. A multi-year study was conducted on a sugarcane operation in Guatemala to investigate this. Due to amorphous silica in sugarcane leaves, amorphous silica has been proposed as a potential exposure. Amorphous silica is heavily under-researched and requires both time and cost-intensive analytical methods that are destructive in nature, resulting in the loss of samples that still require other analyses to be performed on them. This project attempted to address this dilemma by creating a novel non-destructive method using FTIR to generate a predictive model capable of quantitating amorphous silica directly on the filter (DOF Technique). This was the first known attempt at using FTIR outside of mine settings, where NIOSH extensively applies this procedure. Initial results showed promise that the model could be constructed and potentially able to quantitate amorphous silica, however after a method change in the air sampling, the model was unable to quantitate due to a loss in peak signal representative of amorphous silica. Subsequently, we evaluated laboratory filters loaded with known amounts of diatomaceous earth to determine where the machine could not detect amorphous silica. Results from this study demonstrate a higher inconsistency in analysis (i.e., approaching 500 micrograms of amorphous silica). However, several discrepancies in this value require further research to elucidate the true value. This study provides an initial framework to build new DOF techniques outside of a mining setting.

Additionally, this study aimed to provide an increased discussion regarding amorphous silica's potential nephrotoxicity.

5.1 Future Directions

In conducting this project and determining that this pilot was a step forward in determining the risk factors contributing to CKDu, several steps can be taken to advance the research. The first is determining the true distribution of the particles on the filters. As discussed above and as can be seen in Figure 8, there is variation in the absorption peak height at 800 cm^{-1} for each sample. In other words, every filter was analyzed four times in a separate place on the filter. In several instances, such as sample 40 in Figure 8, there is a noticeable difference between the scan at the filter's center versus the scans on the periphery of the filter (i.e., off-center). This result might suggest that variation exists in filter deposition. Future analyses should aim to use the median peak height of the four scans to determine a more appropriate value. Additionally, future aims would be to understand this variability in the deposition of PM onto the filter. Another consideration for future studies includes investigating the difference between using a 37-mm filter with an SKC aluminum cyclone versus using Cauda and colleague's setup which is a smaller 25-mm filter and a Oliver Dorr cyclone (27-29). These two strategies could provide valuable insight into some of the limitations of this project.

6. REFERENCES

1. Johnson, R., Wesseling, C., and Newman, L., *Chronic Kidney Disease of Unknown Cause in Agricultural Communities.* The New England Journal of Medicine, 2019. 380: p. 1843-1852. DOI: 10.1056/NEJMra1813869
2. Butler-Dawson, J., Krisher, L., Asensio, C., Cruz, A., et. al., *Risk Factors for Declines in Kidney Function in Sugarcane Workers in Guatemala.* Journal of Occupational and Environmental Medicine, 2018. 60(6): p. 548-558. DOI: 10.1097/JOM.0000000000001284
3. Paidi, G., Jayarathna, A., Salibindla, D., Ergin, H., et. al., *Chronic Kidney Disease of Unknown Origin: A Mysterious Epidemic.* Cureus, 2021. 13(8): e17132. DOI: 10.7759/cureus.17132
4. Pan-American Health Organzation. *Epidemic of Chronic Kidney Disease in Agricultural Communities in Central America. Case definitions, methodological basis and approaches for public health surveillance.* World Health Organization. [Accessed Jun. 10th, 2023]. https://www.paho.org/en/documents/epidemic-chronic-kidney-disease-agricultural-communities-central-america-case-definitions
5. Ramirez-Rubio, O., McClean, M., Amador, J., and Brooks, D., *An Epidemic of Chronic Kidney Disease in Central America: An Overview.* Journal of Epidemiology and Community Health, 2013. 67(1): p. 1-3. DOI: 10.1136/jech-2012-201141
6. Weiner, D., McClean, M., Kaufman, J., and Brooks, D., *The Central American Epidemic of CKD.* Clinical Journal of the American Society of Nephrology, 2013. 8: p. 504-511. DOI: 10.2215/CJN.05050512
7. Peraza, S., Wesseling, C., Aragon, A., Leiva, Hogstedt, C., et. al., *Decreased Kidney Function Among Agricultural Workers in El Salvador.* American Journal of Kidney Disease, 2012. 59(4): p. 531-540. DOI: 10.1053/j.ajkd.2011.11.039

8. Lunyera, J., Mohottige, D., Von Isenburg, M., and Stanifer, J., *CKD of Uncertain Etiology: A Systematic Review.* Clinical Journal of the American Society of Nephrology, 2016. 11: p. 379-385. DOI: 10.2215/CJN.07500715
9. Orantes, C., Herrera, R., Almaguer, M., and Orellana, P., *Epidemiology of Chronic Kidney Disease in Adults of Salvadoran Agricultural Communities.* MEDICC Review, 2014. 16(2): p. 23-30. DOI: 10.37757/MR2014.V16.N2.5
10. Wesseling, C., Crowe, J., Hogstedt, C., Wegman, D., et. al., *Resolving the Enigma of Mesoamerican Nephropathy: A Research Workshop Summary.* American Journal of Kidney Disease: A Special Report. 2014. 63(3): p. 396-404. DOI: 10.1053:/j.ajkd.2013.08.014
11. Le Blond, J., Williamson, B., Horwell, C., and Oppenheimer, C., *Production of Potentially Hazardous Respirable Silica Airborne Particulate From the Burning of Sugarcane.* Atmospheric Environment, 2008. **142**: p. 5558-55568. DOI: 10.1016/j.atmosenv.2008.03.018
12. Bowe, B., et al., *Estimates of the 2016 Global Burden of Kidney Disease Attributable to Ambient Fine Particulate Matter Air Pollution.* British Medical Journal, 2018. DOI: 10.1136/bmjopen-2018-022450
13. Wu, M., Lo, W., Chao, C., Wu, M., and Chiang, C., *Association Between Air Pollutants and Development of Chronic Kidney Disease: A Systematic Review and Meta-Analysis.* Science of the Total Environment, 2020. **706**: DOI: 10.1016/j.scitotenv.2019.135522
14. Schaeffer, J., Adgate, J., Reynolds, S., Newman, L., et al., *A Pilot Study to Assess Inhalation Exposures Among Sugarcane Workers in Guatemala: Implications for Chronic Kidney Disease of Unknown Origin.* International Journal of Environmental Research and Public Health, 2020. **17**: 5709. DOI: 10.3390//ijerph17165708
15. Sponholtz, T., Sandler, D., Parks, C., and Applebaum, K., *Occupational Exposures and Chronic Kidney Disease: Possible Associations with Endotoxin and Ultrafine Particles.* American Journal of Industrial Medicine, 2015. **59**: p. 1-11 DOI: 10.1002/ajim.22541

16. Prado, G., Zanetta, D., Arbex, M., and Paula Santos, U., *Burnt Sugarcane Harvesting: Particulate Matter Exposure and the Effects on Lung Function, Oxidative Stress, and Urinary 1-hydroxypyrene.* Science of the Total Environment, 2012. **437**: p. 200-208. DOI: 10.1016/j.scitotenv.2012.07.069
17. Le Blond, J., Woskie, S., Horwell, C., and Williamson, B., *Particulate Matter Produced During Commercials Sugarcane Harvesting and Processing: A Respiratory Health Hazard.* Atmospheric Environment, 2017. **149**: p. 34-36. DOI: 10.1016/j.atmosenv.2016.11.012
18. International Agency for Research on Cancer (IARC). *Silica Dust, Crystalline, in the Form of Quartz or Cristabolite.* IARC Monographs on the Evaluation of Carcinogenic Risks to Humans, 100C, 2012. p. 355-405.
19. Warheit, A., *Inhaled Amorphous Silica Particulates: What Do We Know About Their Toxicological Profiles?.* Journal of Environmental Pathology, Toxicology, and Oncology, 2001. **20**: p. 133-141.
20. Stem, A., et. al., *Sugarcane Ash and Sugarcane Ash-derived Silica Nanoparticles Alter Cellular Metabolism in Human Proximal Tubular Kidney Cells.* Environmental Pollution, 2023. **332**: p. 121951 DOI: 10.1016/j.envpol.2023.121951
21. Sasai, F., et al., *Inhaled Silica Nanoparticles Cause Chronic Kidney Disease in Rats.* American Journal of Physiology: Renal Physiology, 2022. **323**(1): p.48-58. DOI: 10.1152/ajprenal.00021.2022
22. Gościcki, J., Woźniak, H., Szendzikowski, S., et al., *Experimental Silicosis. II. Fibrogenic Effect of Natural Amorphous Silica.* Medical Press, 1978. **29**(4): p. 281-291.
23. Occupational Safety and Health Organization (OSHA). *Respirable Crystalline Silica.* 2023. [cited 2023 November 11th]; Available from; https://www.osha.gov/laws-regs/regulations/standardnumber/1926/1926.1153#:~:text=Permissible%20exposure%20limit%20(PEL).,as%20an%208%2Dhour%20TWA.&text=General

24. National Institute for Occupational Safety and Health (NIOSH). *Silica.* 2023. [cited 2023 November 11th]; Available from;
25. National Institute for Occupational Safety and Health (NIOSH). *Silica, Crystalline, by XRD (Filter Redeposition)*. 2003. [cited 2023 November 11th]; Available from; https://www.cdc.gov/niosh/docs/2003-154/pdfs/7500.pdf
26. National Institute for Occupational Safety and Health (NIOSH). *Silica, Amorphous.* CDC.gov. 2003. [cited 2023 November 11th]; Available from; https://www.cdc.gov/niosh/docs/2003-154/pdfs/7501.pdf
27. Cauda, E., Miller, A., and Drake, P., *Promoting Early Exposure Monitoring for Respirable Crystalline Silica: Taking the Laboratory to the Mine Site.* Journal of Occupational and Environmental Hygiene, 2016. **13**(3): p. 39-45. DOI: 10.1080/15459624.2015.1116691
28. National Institute for Occupational Safety and Health (NIOSH). *Quartz in Respirable Coal Mine Dust, by IR (Redeposition).* 2017. [cited 2023 November 11th]; Available from; https://www.cdc.gov/niosh/nmam/pdf/7602.pdf
29. Cauda, E., Chubb, L., Reed, R., and Stepp, R., *Evaluating the Use of a Field-Based Silica Monitoring Approach with Dust from Copper Mines.* Journal of Occupational and Environmental Hygiene, 2018. **15**(10): p. 732-742. DOI: 10.1080/15459624.2018.1495333
30. Kovesdy, P., *Epidemiology of Chronic Kidney Disease Update 2022.* Kidney International Supplements, 2022. **12**(1): p. 7-11. DOI: 10.1016/j.kisu.2021.11.003
31. World Health Organization (WHO). *Global Health Estimates: Life Expectancy and Healthy Life Expectancy.* 2023 [cited 2023 November 11th]; Available from; https://www.who.int/data/gho/data/themes/mortality-and-global-health-estimates/ghe-life-expectancy-and-healthy-life-expectancy#:~:text=The%20estimates%20confirm%20the%20trend,to%2073.4%20years%20in%202019 .

32. Hossain, P., Kawar, B., and Naha, M., *Obesity and Diabetes in the Developing World – A Growing Challenge.* The New England Journal of Medicine, 2007. **356**(3): p. 213-215. DOI: 10.1056/NEJMp068177

33. Jayatilake, N., et al., *Chronic Kidney Disease of Uncertain Aetiology: Prevalence and Causative Factors in a Developing Country.* BioMed Central Nephrology, 2013. **14**(180): DOI: 10.1186/1471-22369-14-180

34. Peraza, S., et al., *Decreased Kidney Function Among Agricultural Workers in El Salvador.* American Journal of Kidney Diseases, 2012. **59**(4): p. 531-540. DOI: 10.1053/j.ajkd.2011.11.039

35. Orantes, C., et al., *Epidemiology of Chronic Kidney Disease in Adults of Salvadoran Agricultural Communities.* MEDICC Review, 2014 **16**(2): p.23-30. DOI: 10.37757/MR2014.V16.N2.5

36. International Society of Nephrology. *What is CKDU.* 2023 [cited 2023 November 11th]; Available from; https://www.theisn.org/initiatives/what-is-ckdu/management/ .

37. Pan-American Health Organization. *Kidney Disease of Unknown Causes in Agricultural Communities in Central America is Declared a Serious Public Health Problem.* 2013. PAHO

38. Hill, N., et al., *Global Prevalence of Chronic Kidney Disease – A systematic Review and Meta-Analysis.* PLoS ONE, 2016. **11**(7): p. e0158765 DOI: 10.1371/journal.pone.0158765

39. Rajapakse, S., Shivantahn, M., and Selvarajah, M., *Chronic Kidney Disease of Unknown Etiology in Sri Lanka.* International Journal of Occupational and Environmental Health, 2016. **22**(3): p. 259-264. DOI: 10.1080/10773525.2016.1203097

40. Wimalawansa, S., *Public Health Interventions for Chronic Disease: Cost-Benefit Modelizations for Eradicating Chronic Kidney Disease of Multifactorial Origin (CKDmfo/CKDu) from Tropical Countries.* Heliyon, 2019. DOI: 10.1016/j.heliyon.2019.e02309

41. Alwis, A., and Panawala, P., *A Review of the National Response to CKDu in Sri Lanka.* Sri Lanka Journal of Social Sciences, 2019. **42**(2): p. 83-100. DOI: 10.4038/sljss.v42i2.7966
42. Kulathunga, M., Wijayawardena, M., Naidu, R., and Wijeratne, A., *Chronic Kidney Disease of Unknown Aeteiology in Sri Lanka and the Exposure to Environmental Chemicals: A Review of Literature.* Environmental and Geochemical Health, 2019. **41:** p.2329-2338. DOI: 10.1007/s10653-019-00264
43. Wesseling, C., *Is an Environmental Nephrotoxin the Primary Cause of CKDu (Mesoamerican Nephropathy)? CON.* Kidney360, 2020 **1**: p. 596-601. DOI: 10.34067/KID.0002922020
44. Wesseling, C., et. al., *Mesoamerican Nephropathy: Geographical Distribution and Time Trends of Chronic Kidney Disease Mortality Between 1970 and 2012 in Costa Rica.* Occupational and Environmental Medicine, 2015. **72**: p. 714-721. DOI: 10.1136/oemed-2014-102799
45. DeBroe, M., and Vervaet, B., *Is an Environmental Nephrotoxin the Primary Cause of CKDu (Mesoamerican Nephropathy)? PRO.* Kidney360, 2020 **1**: p. 591-595. DOI: 10.34067/KID.0003172020
46. Lin, S., et al. *Air Pollutants and Subsequent Risk of Chronic Kidney Disease and End-Stage Renal Disease: A Population-Based Cohort Study.* Environmental Pollution, 2019. **261**: DOI: 10.1016/j.envpol.2020.114514
47. Afsar, B., et al., *Air Pollution and Kidney Disease: A Review of Current Evidence.* Clinical Kidney Journal, 2019. **12**(1): p. 19-32. DOI: 10.1093/ckj/sfy111
48. Bowe, B., et al., *Associations of Ambient Coarse Particulate Matter, Nitrogen Dioxide, and Carbon Monoxide with the Risk of Kidney Disease: A Cohort Study.* The Lancet: Planetary Health, 2017. **1**. p. 267-276. DOI: 10.1016/S2542-5196(17)30117-1

49. Chan, T., Zhang, Z., Lin, B., Lin, C., Lao, X., et al. *Long-Term Exposure to Ambient Fine Particulate Matter and Chronic Kidney Disease: A Cohort Study.* Environmental Health Perspectives, 2018. **126**(10) DOI: 10.1289/EHP3304

50. Liu, B., Fan, D., Huang, F., *Relationship of Chronic Kidney Disease with Major Air Pollutants – A Systematic Review and meta-Analysis of Observational Studies.* Journal of Environmental Toxicology and Pharmacology, 2020. **76**: DOI:10.1016/j.etap.2020.103355

51. Yangjie, L., Kolasinski, K., and Zare, R., *Silica Particles Convert Thiol-Containing Molecules to Disulfides.* Proceedings for the National Academy of Sciences (PNAS), 2023. **120**(34): p. e2304735120. DOI: 10.1073/pnas.2304735120

52. Hart, J., et al., *A Comparison of Respirable Crystalline Silica Concentration Measurements Using a Direct-On-Filter Fourier Transform Infrared (FT-IR) Transmission Method vs. A Traditional Laboratory X-Ray Diffraction Method.* Journal of Occupational and Environmental Hygiene, 2018. **15**(10): p. 743-754. DOI: 10.1080/15459624.2018.1495334

53. Ojima, J., *Determining of Crystalline Silica in Respirable Dust Samples by Infrared Spectroscopy in the Presence of Interferences.* Journal of Occupational Health, 2003. **45**: p. 94-103. DOI: 10.1539/joh.45.94

7. APPENDICES

Appendix A

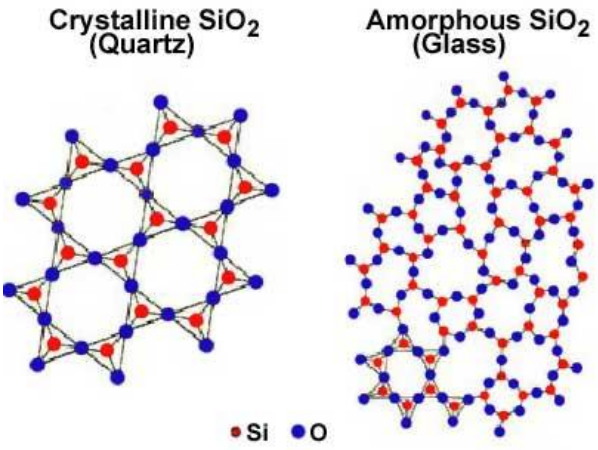

Diagram 1: Chemical structure of Crystalline Silica (on left) vs. Amorphous Silica (on right). Blue represents oxygen molecules and red represents silicon molecules. Diagram obtained from https://physicsopenlab.org/2018/02/13/crystalline-and-amorphous-solids/

Appendix B

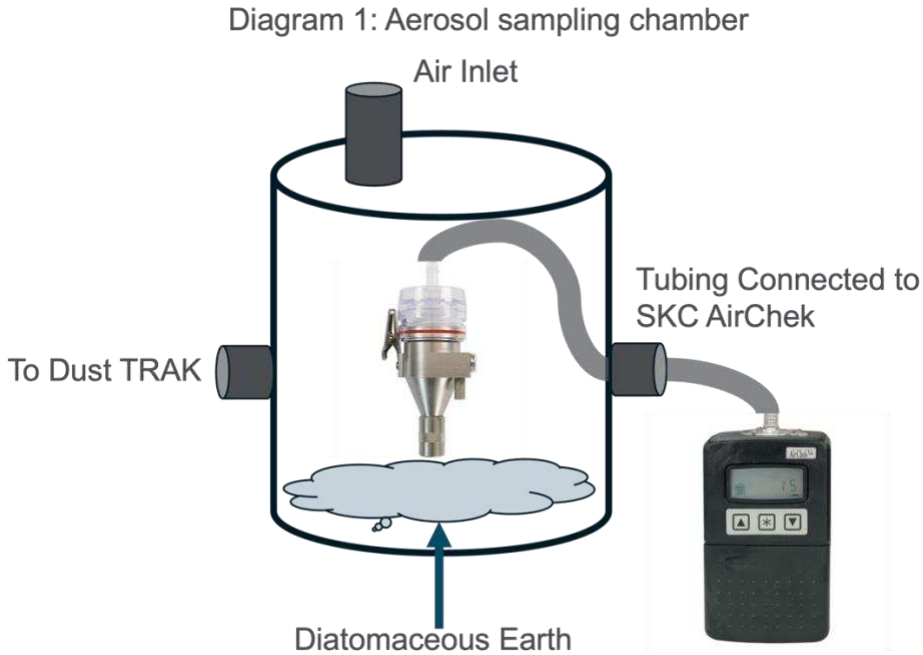

Diagram 2: Schematic of aerosol sampling chamber used in the lab loading study. The BGI Cyclone was placed inside the chamber with the tubing attached to the air pump running through a secure hose connector. Diatomaceous Earth was loaded into the chamber at the bottom and an air tube was attached to the system to input air and quick bursts were used to generate dust that could be collected.

Appendix C

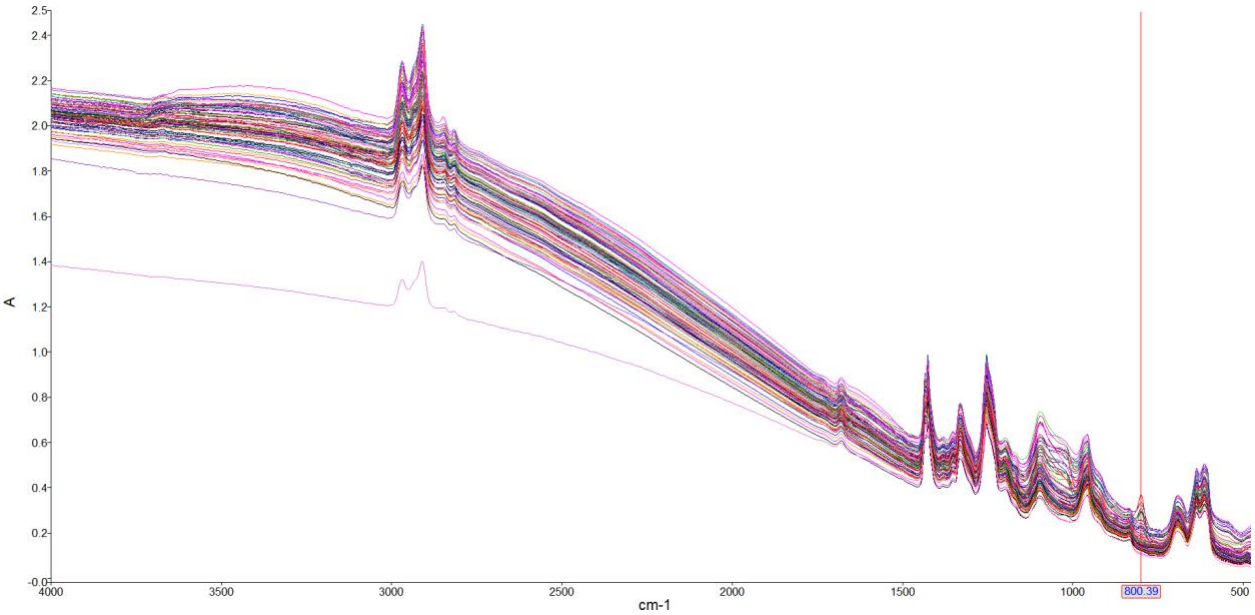

Figure 8: Full PPI spectrum obtained from the pilot study

Appendix D

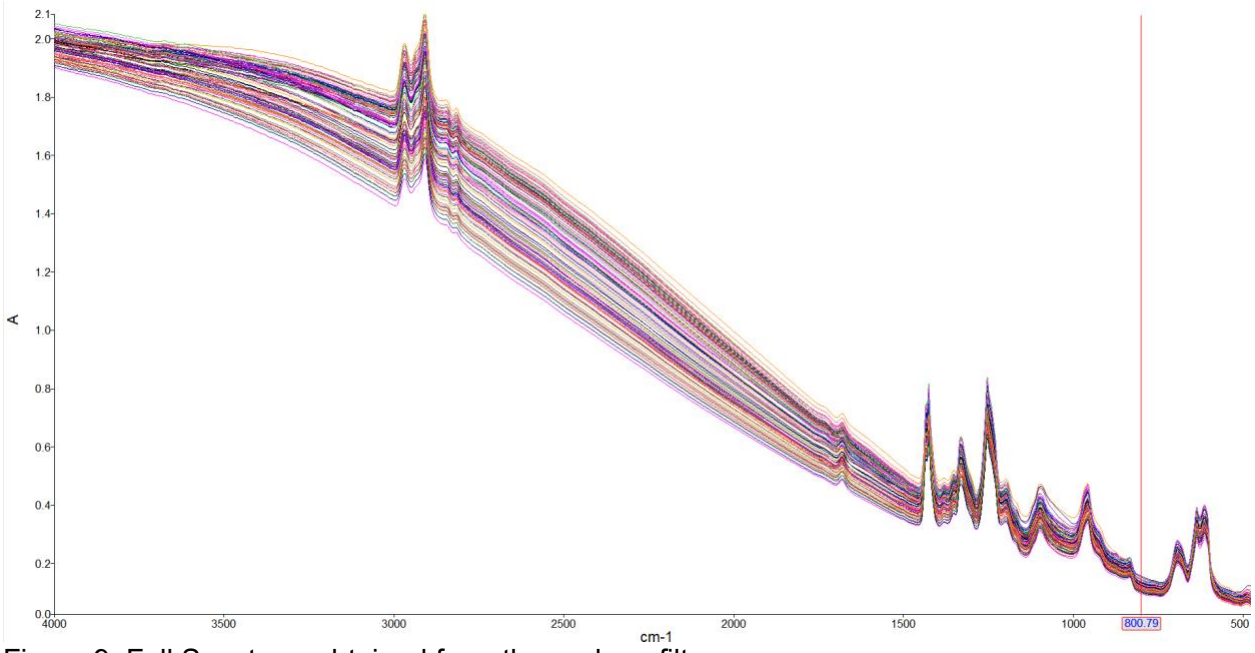

Figure 9: Full Spectrum obtained from the cyclone filters